Environmental Science & Technology

Article

pubs.acs.org/est

Biotransformation of Two Pharmaceuticals by the Ammonia-Oxidizing Archaeon *Nitrososphaera gargensis*

Yujie Men,[*,†,‡] Ping Han,[§] Damian E. Helbling,[∥] Nico Jehmlich,[⊥] Craig Herbold,[§] Rebekka Gulde,[†] Annalisa Onnis-Hayden,[#] April Z. Gu,[#] David R. Johnson,[†] Michael Wagner,[§] and Kathrin Fenner[†,⊗]

[†]Eawag, Swiss Federal Institute of Aquatic Science and Technology, 8600 Dübendorf, Switzerland

[‡]Department of Civil and Environmental Engineering, University of Illinois at Urbana−Champaign, Urbana, Illinois 61801, United States

[§]Department of Microbiology and Ecosystem Science, Division of Microbial Ecology, Research Network "Chemistry meets Microbiology", University of Vienna, Althanstrasse 14, 1090 Vienna, Austria

[∥]School of Civil and Environmental Engineering, Cornell University, Ithaca, New York 14853, United States

[⊥]Department of Proteomics, Helmholtz-Centre for Environmental Research − UFZ, 04318 Leipzig, Germany

[#]Department of Civil and Environmental Engineering, Northeastern University, Boston, Massachusetts 02115, United States

[⊗]Department of Environmental Systems Science, ETH Zürich, 8092 Zürich, Switzerland

Supporting Information

ABSTRACT: The biotransformation of some micropollutants has previously been observed to be positively associated with ammonia oxidation activities and the transcript abundance of the archaeal ammonia monooxygenase gene (*amoA*) in nitrifying activated sludge. Given the increasing interest in and potential importance of ammonia-oxidizing archaea (AOA), we investigated the capabilities of an AOA pure culture, *Nitrososphaera gargensis*, to biotransform ten micropollutants belonging to three structurally similar groups (i.e., phenylureas, tertiary amides, and tertiary amines). *N. gargensis* was able to biotransform two of the tertiary amines, mianserin (MIA) and ranitidine (RAN), exhibiting similar compound specificity as two ammonia-oxidizing bacteria (AOB) strains that were tested for comparison. The same MIA and RAN biotransformation reactions were carried out by both the AOA and AOB strains. The major transformation product (TP) of MIA, α-oxo MIA was likely formed via a two-step oxidation reaction. The first hydroxylation step is typically catalyzed by monooxygenases. Three RAN TP candidates were identified from nontarget analysis. Their tentative structures and possible biotransformation pathways were proposed. The biotransformation of MIA and RAN only occurred when ammonia oxidation was active, suggesting cometabolic transformations. Consistently, a comparative proteomic analysis revealed no significant differential expression of any protein-encoding gene in *N. gargensis* grown on ammonium with MIA or RAN compared with standard cultivation on ammonium only. Taken together, this study provides first important insights regarding the roles played by AOA in micropollutant biotransformation.

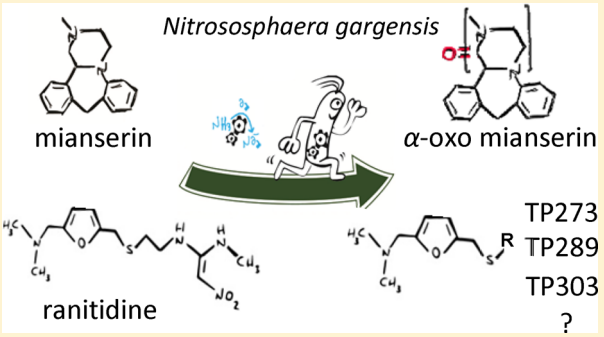

INTRODUCTION

In recent years, increasing concerns have arisen about emerging contaminants in aquatic systems, such as pesticides, pharmaceuticals, and personal care products due to their potential adverse effects on ecosystems and public health.[1,2] These compounds are sometimes referred to as micropollutants (MPs) because they are typically detected at ng−μg/L levels. A systematic and mechanistic understanding of how MPs are mitigated and transformed in receiving environments is needed to help assess the environmental persistence and ecotoxicity of the MPs and their subsequent transformation products, which can then guide the establishment of corresponding remediation strategies or environmental regulations.[3] Biotransformation plays an important role in the environmental fate of MPs, particularly in wastewater treatment plants (WWTPs), a major sink for down-the-drain chemicals.

A number of studies have demonstrated significant associations between MP biotransformation and nitrification activities. Enhanced biotransformation was observed for a variety of MPs, including pharmaceuticals, pesticides, and estrogens, as higher ammonia oxidation activities were reached in nitrifying activated sludge (NAS).[4,5] Consistently, MP biotransformation declined when nitrification was inhibited by

Received: December 8, 2015
Revised: March 25, 2016
Accepted: April 5, 2016
Published: April 5, 2016

DOI: 10.1021/acs.est.5b06016
Environ. Sci. Technol. 2016, 50, 4682−4692

allylthiourea (ATU), a commonly used ammonia monooxygenase (AMO) inhibitor.[6−10] It was then hypothesized that AMO in ammonia-oxidizing microorganisms (AOMs) were involved in the MP biotransformation, most likely by cometabolism.[9,10] Studies on isolates of ammonia-oxidizing bacteria (AOB) revealed cometabolic biotransformation activities for estrogens, polycyclic aromatic hydrocarbons, and pharmaceutical compounds.[9−13] One exception is *Nitrosomonas eutropha* C91, which was found to degrade metabolically *p*-cresol and use the intermediates as energy source via mixtrophy instead of cometabolism.[14] Helbling et al.[15] carried out a systematic analysis on the association between WWTP parameters and the biotransformation of a diverse set of MPs. They observed that the oxidation rates of four N-containing compounds (i.e., isoproturon, valsartan, venlafaxine, and ranitidine) were significantly associated with effluent ammonia concentrations and ammonia removal. Notably, by analyzing bacterial and archaeal *amoA* gene expression in the activated sludge communities during MP biotransformation, they also noticed that the transcript abundance of archaeal *amoA* rather than bacterial *amoA* showed a significant positive association with the biotransformation of isoproturon, venlafaxine, and ranitidine. When the ammonia oxidizers were inhibited by acetylene, isoproturon biotransformation was inhibited, but no significant effect was observed for the other compounds.[15] These results suggest that ammonia-oxidizing archaea might have MP biotransformation potential besides their remarkable role in the global biogeochemical nitrogen cycle.

Ammonia oxidizers in municipal WWTPs are generally dominated by AOB,[16,17] but high abundances of AmoA-encoding archaea (AEA) have been reported in some municipal and industrial WWTPs using archaeal *amoA* gene as a biomarker.[18,19] However, not all AEA necessarily oxidize ammonium, as the AMO belongs to an enzyme family known to be substrate promiscuous.[20] Furthermore, AEA might be physiologically versatile and ammonia oxidation might be one of several lifestyles of these organisms. Indeed, in an industrial WWTP with high AEA abundance it has been demonstrated that these archaea obtain energy from substrates other than ammonia.[20] Archaeal AMO has a significantly higher ammonia affinity than bacterial AMO. The half-saturation constants (Km) of ammonia for archaeal AMO were found to be at the nM level, which is 100 times lower than those for bacterial AMO (in μM).[21] Given the low concentrations of MPs (in the pM−nM range) and the relatively high concentrations of ammonia (in mM) in WWTPs, the difference in substrate affinity of archaeal and bacterial AMO suggests that AOA might be even more important for biotransforming MPs in WWTPs than AOB, which would be consistent with the previously observed correlation between the biotransformation of some MPs and transcript abundance of archaeal *amoA* but not bacterial *amoA*.[15] In contrast, AOB tend to be more competitive in ammonia oxidation over AOA in WWTPs. However, to address whether AOA can contribute to MP removal, targeted studies with AOA pure cultures and nitrifying sludge community studies are required. Previous studies have mainly focused on the roles played by AOB in MP biotransformation, and to our knowledge MP biotransformation capabilities of AOA strains have not yet been reported.

The goal of this study was to address this knowledge gap by investigating the capabilities of MP biotransformation by *Nitrososphaera gargensis*, one of the few available AOA pure cultures,[22,23] as well as elucidating possible transformation reactions through the analysis of transformation products (TPs). AOA pure cultures isolated from WWTPs are not yet available. Although *N. gargensis* is a moderate thermophile that was isolated from an outflow of a hot spring, it is phylogenetically closely related to AOAs typically found in WWTPs.[19,24] Biotransformation of ten MPs by *N. gargensis* was investigated. These MPs included the four compounds whose biotransformation was previously shown to be associated with ammonia removal and/or archaeal *amoA* transcript abundances, as well as six other structurally similar compounds from three categories: phenylureas, tertiary amides, and tertiary amines. Biotransformation of the ten selected compounds by *N. gargensis* and two AOB strains were examined. Major transformation products (TPs) were identified and possible biotransformation pathways were proposed. Whether the biotransformed compounds can serve as an energy source was also tested to determine whether their biotransformation was via a metabolic or cometabolic pathway.

MATERIALS AND METHODS

MP Selection. The ten selected MPs are from three structurally similar groups: phenylureas, tertiary amides, and tertiary amines (Table S1). They include the four compounds (i.e., isoproturon, valsartan, venlafaxine, and ranitidine) whose biotransformation rates were found to associate positively with ammonia oxidation activity of activated sludge communities or archael *amoA* transcript abundances.[15] Another six compounds were selected based on structural similarity with the previous four compounds, and other criteria including (1) minimal number of readily biotransformed functional groups other than the three focused ones and (2) widely used pesticides and pharmaceuticals with reference standards available. The ten parent compounds, and literature-reported TPs (Table S1) of mianserin (MIA) and ranitidine (RAN), as well as the analogue compounds used for analyzing the structure of the major MIA TP (i.e., mirtazapine, analogue of MIA; 1-oxo mirtazapine, and 10-oxo mirtazapine, analogues of the major MIA TP) were purchased from Sigma-Aldrich Chemie GmbH (Buchs, Switzerland), Dr. Ehrenstorfer GmbH (Augsburg, Germany), and Toronto Research Chemicals (Toronto, Canada). Stock solutions of each reference compound were prepared in methanol or ethanol (1 g/L), and stored at −20 °C until use.

Cultivation of Ammonia-Oxidizing Microbes. The AOA strain, *N. gargensis*, was cultivated in a modified basal medium[23] with 8 g/L $CaCO_3$ for buffering the pH at ∼8.0. The culture was incubated in the dark without shaking. 2 mM NH_4Cl was added as growth substrate every 6 days. Two AOB strains isolated from WWTPs, *Nitrosomonas nitrosa* Nm90[25] and *Nitrosomonas* sp. Nm95, were obtained from the AOB strain collection of the University of Hamburg (Germany)[25] and were maintained in 50 mL suspension culture flasks (Bartelt GmbH), in the dark with shaking at 80 rpm, using the same basal medium amended with 10 mM NH_4Cl every 2 weeks. *N. gargensis* was incubated at 46 °C and the two AOB strains were incubated at 28 °C, which are considered their optimal temperatures for growth. The purity of *N. gargensis* was confirmed by a negative PCR result using universal bacterial 16S rRNA gene primers. The purity of the two AOB cultures was confirmed by no detection of contaminant 16S rRNA gene sequences from 16S rRNA gene amplicon sequencing results (data not shown).

DOI: 10.1021/acs.est.5b06016
Environ. Sci. Technol. 2016, 50, 4682−4692

Table 1. First-Order Biotransformation Rate Constants (k_{bio}) of MIA and RAN by *N. gargensis* and the Two AOB Strains

culture	NO_2^- formation rate[a] ($mM \cdot d^{-1}$)	total protein[a] ($mg \cdot L^{-1}$)	k_{bio}[b] [$L \cdot (mg\ total\ protein)^{-1} \cdot d^{-1}$]		k_a[b] (d^{-1})		K_d[b] [$L \cdot (mg\ total\ protein)^{-1}$]	
			MIA	RAN	MIA	RAN	MIA	RAN
N. gargensis (with 2 mM NH_4–N and ten MPs, 40 $\mu g/L$ each)	0.74 ± 0.12	28.2 ± 1.0	0.018 [0.017, 0.022]	0.0073 [0.0063, 0.0089]	0.011 [0.001, 0.026]	0.0036 [0, 0.013]	0.0011 [0, 0.005]	0.0025 [0, 0.0098]
N. gargensis (with 2 mM NH_4–N and 40 $\mu g/L$ MIA/RAN)	0.85 ± 0.11 (+MIA)	26.8 ± 1.3 (+MIA)	0.025 [0.021, 0.031]	0.0071 [0.0059, 0.0092]	0.086 [0.057, 0.12]	0.016 [0.004, 0.03]	0.0011 [0, 0.005]	0.0026 [0, 0.013]
	0.63 ± 0.19 (+RAN)	27.8 ± 0.6 (+RAN)						
N. gargensis (with 2 mM NH_4–N and 100 $\mu g/L$ MIA/RAN)	0.88 ± 0.06 (+MIA)	15.0 ± 0.8 (+MIA)	0.068 [0.054, 0.093]	0.0059 [0.0013, 0.011]	N/A	N/A	N/A	N/A
	0.22 ± 0.06 (+RAN)	14.4 ± 0.8 (+RAN)						
N. gargensis (with 0.2 mM NH_4–N and 100 $\mu g/L$ MIA/RAN)	N/A	14.0 ± 0.2 (+MIA)	N/A	N/A	N/A	N/A	N/A	N/A
		14.0 ± 0.4 (+RAN)						
N. nitrosa Nm90 (with 2 mM NH_4–N and ten MPs, 40 $\mu g/L$ each)	0.39 ± 0.02	8.4 ± 0.4	0.016 [0.011, 0.023]	0.0027 [0.0023, 0.0034]	0.079 [0.057, 0.10]	0.00077 [0, 0.002]	0.0083 [0, 0.039]	0.0078 [0, 0.036]
Nitrosomonas sp. Nm95 (with 2 mM NH_4–N and ten MPs, 40 $\mu g/L$ each)	0.98 ± 0.09	10.2 ± 0.1	0.001 [0.0002, 0.0027]	0.0015 [0.0011, 0.0018]	0.025 [0.011, 0.035]	0.0022 [0, 0.0053]	0.0090 [0.001, 0.034]	0.0027 [0.0013, 0.0050]
N. gargensis (with 2 mM NH_4–N only)	0.83 ± 0.17	29.7 ± 1.2						
N. gargensis (with 0.2 mM NH_4–N only)	N/A	14.4 ± 0.4			N/A			
N. nitrosa Nm90 (with 2 mM NH_4–N only)	0.61 ± 0.03	7.8 ± 0.4						
Nitrosomonas sp. Nm95 (with 2 mM NH_4–N only)	1.09 ± 0.10	10.0 ± 0.5						

[a]Average ± standard deviation of triplicates. [b]Normalized to total protein; values are reported as median with 5%, 95% percentile in brackets.

DOI: 10.1021/acs.est.5b06016
Environ. Sci. Technol. 2016, 50, 4682–4692

Biotransformation by AOA and AOB. MP biotransformation capabilities of the AOA and AOB strains were investigated in batch cultures. Pregrown biomass was harvested by centrifugation at 8500 rpm at 4 °C for 30 min, then resuspended in fresh medium to remove residual nitrite and to concentrate the biomass by about 4−6 times, resulting in an ammonia turnover rate of the concentrated biomass at ∼1 mM per day. To avoid potential inhibitory effects of methanol or ethanol in the MP stock solutions to AOA/AOB cultures, certain volumes of individual MP or mixed MP stock solution (100 mg/L of each compound) to make a start concentration of 40 μg/L for each MP was first added into empty sterile bottles. After the organic solvents were evaporated, 50 or 25 mL of thoroughly mixed concentrated AOA/AOB culture was inoculated into 100 mL Schott glass bottles or 50 mL suspension culture flasks, respectively. The bottles were loosely capped and shaken at 160 rpm for ∼20 min to redissolve the MPs. NH_4Cl was added afterward to a start concentration of 2 mM and was readded to 2 mM when it was below 1 mM. This concentration is much higher than typical half-saturation constants of AOA and at least 5 times higher than those of AOB.[21,26] Thus, ammonia was considered unlimited with semicontinuous reamendment and the ammonia turnover rate was nearly constant during the incubation period. Nitrite did not accumulate above 10 mM and showed no inhibition of ammonia oxidizing activity at these concentrations (data not shown). The bottles were incubated at the optimal growth temperatures for the tested AOA and AOB strains, respectively. Samples (∼1 mL) were taken immediately after ammonium addition. Of the 1 mL sample, 0.2 mL was stored at −20 °C for qPCR analysis, and the rest was centrifuged at 11,000 rpm at 4 °C for 15 min. About 0.6 mL of supernatant was transferred into 2 mL amber glass vials and stored at 4 °C in the dark until LC-MS/MS analysis (max. 14 days of storage until analysis). The remaining supernatant was transferred into 1.5 mL microcentrifuge tubes and stored at 4 °C for ammonia and nitrite measurements. The cell pellets were stored at −20 °C for total protein measurement. Subsequent samples were taken in the same way at 2, 8, 24, 48, 72, 96, and 125 h. Samples at later time points (i.e., 7, 10, and 18 d) were also taken for experiments performed with the two AOB strains.

The sorption potential of MPs to the medium matrix containing $CaCO_3$ precipitates was examined by conducting abiotic control experiments with fresh medium containing either 48 g/L or no $CaCO_3$. Samples were taken at 2, 24, 48, 72, and 125 h (SI section S2). In addition, control experiments with dead microbial biomass were set up in the same way as the biotransformation reactors. For this purpose, the biomass was autoclaved twice at 121 °C and 103 kPa for 20 min. 2 mM ammonium and 6 mM nitrite were added into sorption and heat-inactivated samples to mimic the N levels in the biological samples and investigate possible abiotic transformation in the presence of ammonium and nitrite. Samples were taken at multiple time points during the same incubation period as for the biotransformation reactors. All experiments were performed in triplicates.

Metabolic or Cometabolic Biotransformation. Whether MIA or RAN was metabolically utilized by *N. gargensis* was tested separately using the same setup, but with a minimal NH_4−N concentration (0.2 mM, without reamendment) as nitrogen source only (denoted "Lo_NH_4-N") and 100 μg/L MP as the potential energy source. Batch cultures amended with sufficient NH_4−N (2 mM, with reamendment) and 100 μg/L MP were used as positive controls (denoted "Hi_NH_4-N"). Samples were taken over a time course of 10 and 16 d for the Hi_NH_4-N and Lo_NH_4-N reactors, respectively.

Estimation of Kinetic Parameters. Given that the growth substrate ammonium was unlimited, the cometabolic reductant and competition models could theoretically be simplified to a first-order model (Table S3 and see details in SI section S4). To compare quantitatively biotransformation activities among biological samples, we estimated biotransformation rate constants (k_{bio}) for MIA and RAN normalized to total protein (Table 1) by using a first-order model (eqs 1−3) described previously, which incorporates sorption, abiotic transformation, and biotransformation processes.[27,28] A Bayesian fitting procedure was used for parameter estimation as described elsewhere.[27] The median value calculated from the fitting procedure was used as the estimated k_{bio}, with the 5% and 95% percentile values representing the estimation uncertainty. The fitting quality was evaluated by plotting measured data against model predictions including 90% credibility intervals and by the root-mean-square errors (Figure S7).

$$\frac{dS_c}{dt} = -f_{aq}(k_{bio}X + k_a)S_c \quad (1)$$

$$f_{aq} = \frac{S_c}{S_{ct}} \quad (2)$$

$$K_d = \frac{1 - f_{aq}}{f_{aq}X} \quad (3)$$

where S_c is the aqueous concentration of the compound, f_{aq} is the dissolved compound fraction, k_{bio} is the total protein concentration-normalized biotransformation rate constant, X is the total protein concentration, k_a is the abiotic transformation rate, S_{ct} is the total concentration of the compound, and K_d is the sorption coefficient.

Analytical Methods. Compound concentrations were analyzed by reversed phase liquid chromatography coupled to a high-resolution quadrupole orbitrap mass spectrometer (LC-MS/MS) (Q Exactive, Thermo Fisher Scientific Corporation, San Jose, US). To eliminate the interference of mineral salts and phosphate contained in the medium, an automated online solid phase extraction (online SPE) was applied prior to LC-MS/MS according to the method setup described previously.[29,30] The detailed method is described in SI section S1. Briefly, samples or standards were diluted in nanopure water by 100 times to a total volume of 20 mL with the addition of internal standards (400 ng/L each, Table S2). The 20 mL sample was loaded onto a customized extraction cartridge. The enriched sample was then loaded on an XBridge C_{18} HPLC column (particle size 3.5 μm, 2.1 × 50 mm, Waters), eluted using a gradient of nanopure water (Barnstead Nanopure, Thermo Scientific) and methanol (HPLC-grade, Fisher Scientific), both amended with 0.1% (v/v) formic acid (98−100%, Merck). The MS detection was done by full scan acquisition (resolution of 140 000 at 200 m/z, a range of 100−550 m/z) in electrospray ionization (ESI) positive mode. Calibration curves were established using standard series (1−750 ng/L in 20 mL, with 400 ng/L internal standards). The lowest calibration point was regarded as the limit of quantification (LOQ).

Transformation Product Identification. Suspect screening was used to identify potential transformation products (TP)

DOI: 10.1021/acs.est.5b06016
Environ. Sci. Technol. 2016, 50, 4682−4692

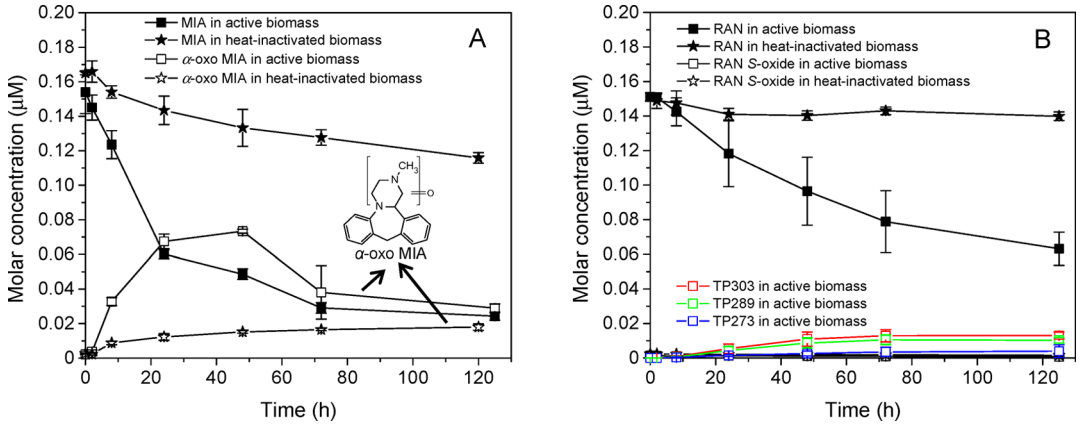

Figure 1. Biotransformation and TP formation of MIA (A) and RAN (B) by active and heat-inactivated biomass of *N. gargensis* (note: concentrations of α-oxo MIA, RAN_TP303, TP289, and TP273 were estimated using peak areas and calibration curves of the corresponding parent compounds assuming that TPs have the same ionization efficiency as their parent compounds; Formation of RAN_TP303, TP289, and TP273 in heat-inactivated biomass was negligible and not shown).

formed during MIA and RAN biotransformation by the ammonia oxidizers.[31] Suspect lists of potential TPs for MIA and RAN were compiled using a self-written, automated metabolite mass prediction script taking into account a variety of known redox and hydrolysis reactions, as well as conjugation reactions. It was then imported to TraceFinder 3.1 (Thermo Scientific) as the compound database for a TP suspect screening method. The exact masses of [M + H] for suspected TPs were extracted from the high resolution, MS full-scan. Those that had 10% of the peak area of the parent compound (>10^7 in peak areas), >70% match with the predicted isotopic pattern, and an increasing trend over the time course were subjected to further identification.

Because no TP candidate for RAN was identified from suspect screening, nontarget screening was further carried out to find possible RAN TPs. Sieve 2.2 (Thermo Scientific) was used for nontarget screening. TP candidates were selected based on the following criteria: (i) intensity above a set threshold with reasonable peak shape; (ii) presence in RAN-added samples and absence in MIA-added samples and heat-inactivated controls; (iii) TP-like time-series pattern (i.e., increase or increase and decrease over the time course of experiment); (iv) a reasonable chemical formula derived from the exact mass of [M + H] and isotopic pattern. Identified TP candidate peaks were integrated using Xcalibur 2.2 (Thermo Scientific).[32]

To elucidate structures of all identified TP peaks from suspect and nontarget screening, additional MS^2 measurements were conducted later with a Q Exactive instrument (Thermo Scientific) and MS^3 measurements on Orbitrap XL (Thermo Scientific). Details are described in SI section S6. MarvinSketch (NET6.2.0, 2014) was used for drawing, displaying and characterizing chemical structures, ChemAxon (http://www.chemaxon.com).

As the reference compounds for MIA and RAN TP candidates were not commercially available, to do a relative comparison, they were semiquantified with peak areas and calibration curves of the corresponding parent compounds assuming that the TP(s) and the parent compound have the same ionization efficiency.

Ammonium and Nitrite Measurements. Nitrite was measured by photometry with the sulfanilamide *N*-(1-naphthyl)ethylenediamine dihydrochloride (NED) reagent method.[33] Ammonium (NH_4^+ + NH_3) were measured by a colorimetric method as described previously.[34]

Total Protein Measurement. Total protein was measured using a Pierce BCA Protein Assay Kit (Thermo Scientific, Regensburg, Germany) according to the manufacturer's instructions.

Quantitative PCR. *N. gargensis* 16S rRNA gene copy numbers were measured by quantitative PCR (qPCR) using specific primer sets, forward (NG1052) 5′-TAGTTGCT-ACCTCTGTTC-3′, reverse (NG1436R) 5′-ACCTTGTT-ACGACTTCTC-3′, as described elsewhere.[23] Each qPCR reaction was performed in a 20 μL reaction mix containing 10 μL of SYBR Green Supermix, 0.1 μL of 50 μM each primer, 7.9 μL of autoclaved double-distilled ultrapure water, and 2 μL of the sampled *N. gargensis* cell suspension, which was subjected to lysis during the 10 min denaturing step at 95 °C prior to 43 PCR cycles of 40 s at 94 °C, 40 s at 55 °C, and 45 s at 72 °C. Plasmids carrying the *N. gargensis* 16S rRNA gene were obtained by cloning the PCR product into a pCR4-TOPO TA vector (Invitrogen). The PCR product reamplified using M13 primers from these plasmids was quantified with PicoGreen reagents under a fluorospectrometer and used as qPCR standard. 10-fold serial dilutions of the standard were used to generate an external calibration curve. The qPCR reactions were performed with three technical replicates in a Bio-Rad C1000- CFX96 Real-Time PCR system, using the Bio-Rad iQ SYBR Green Supermix kit (Bio-Rad) according to the manufacturer's instructions.

Proteomic Analysis. *N. gargensis* was inoculated into triplicate bottles after the addition of 40 μg/L MIA, RAN, and venlafaxine (nonbiotransformed control), respectively as described above. Bottles with no MP addition were used as controls. NH_4Cl (2 mM) was added into each bottle as the growth substrate. Cells were harvested after 48 h by centrifugation at 11,000 rpm at 4 °C for 15 min. Proteins were extracted from the cell pellets and separated on 1D-separation SDS-PAGE. One broad band of the loading protein sample was then subjected to proteolytic cleavage into peptides. Proteomic analyses of *N. gargensis* were performed by loading the peptide lysates on UHPLC-MS (Orbitrap Fusion, Thermo Fisher Scientific). More details on the proteomic analyses are provided in SI section S7.

DOI: 10.1021/acs.est.5b06016
Environ. Sci. Technol. 2016, 50, 4682−4692

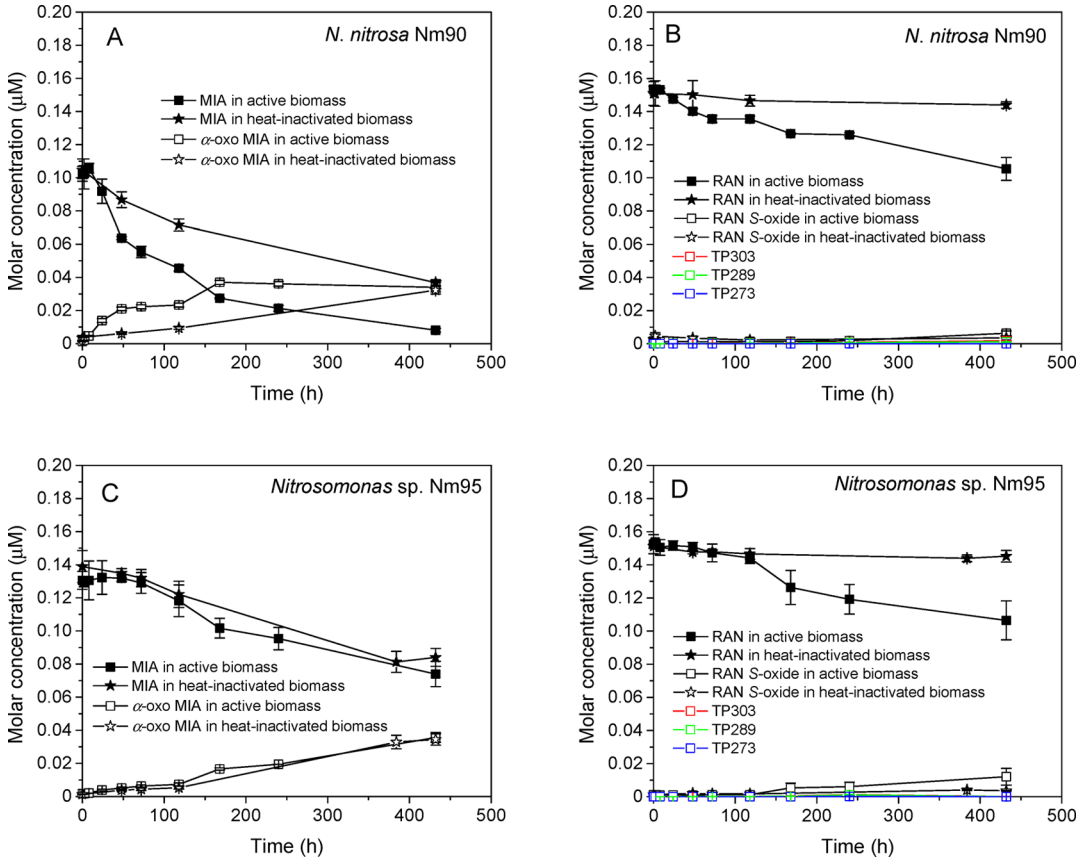

Figure 2. Biotransformation and TP formation of MIA and RAN by active and heat-inactivated biomass of *N. nitrosa* Nm90 (A,B) and *Nitrosomonas* sp. Nm95 (C,D) (note: concentrations of α-oxo MIA, RAN_TP303, TP289, and TP273 were estimated using peak areas and calibration curves of the corresponding parent compounds assuming that TPs have the same ionization efficiency as their parent compounds; formation of RAN_TP303, TP289, and TP273 in heat-inactivated biomass was negligible and not shown).

The acquired MS spectra were processed in Proteome Discoverer (v1.4.1.14, Thermo Scientific) and aligned against a *N. gargensis* database (Uniprot/Swiss-Prot, containing 3786 unreviewed sequence entries) using the Sequest HT algorithm. Protein abundances were $\log_{10}$ transformed and median normalized. The differential proteomic analysis was performed using a two-sample *t* test (equal variance), corrected with the Benjamini–Hochberg method at false discovery rate (FDR) < 0.05. Partial least-squares regression (PLS) was used to examine the holistic proteomic profiles of all *N. gargensis* samples. The details are described in SI section S7.

RESULTS AND DISCUSSION

MP Biotransformation by AOA and AOB Strains. First of all, sorption of the ten tested MPs to $CaCO_3$ precipitates was examined, as well as abiotic transformation of the MPs in autoclaved fresh medium. No significant sorption was observed. Depending on the compound, 0–22% of the added MP was abiotically removed during an incubation time of 120 h (Figure S1). Next, the MP biotransformation capabilities of the tested AOA and AOB strains were screened. Compared to the control with heat-inactivated biomass, significant removal (end time point, two-tailed *t* test, $p < 0.05$) of MIA and RAN by the AOA *N. gargensis* (Figure 1) and the AOB *N. nitrosa* Nm90 (Figure 2A,B) was observed. *Nitrosomonas* sp. Nm95 also removed RAN (Figure 2D), but the MIA removal was similar to that in the heat-inactivated biomass (Figure 2C). Some removal of MIA was observed in all controls with heat-inactivated biomass, but this effect was clearly higher in the heat-inactivated MIA-biotransforming *N. gargensis* and *N. nitrosa* Nm90 (120 h removal ~ 30%) than in the heat-inactivated non MIA-biotransforming *Nitrosomonas* sp. Nm95 and the biomass-free medium control (120 h removal ~ 10%) (SI section S2 and Figure S2). This suggests that some enzymatic MIA-transforming activity remained in the heat-inactivated biomass of *N. gargensis* and *N. nitrosa* Nm90 that biotransformed MIA during active growth. Nevertheless, no ammonia oxidation activity was observed in the heat-inactivated biomass (Figure S3), leaving the exact reason for this effect unclear. There was no biotransformation activity for the other eight tested MPs, as the overall removals were <10% in active biomass samples and similar to those in the heat-inactivated control (Figures S4–S6).

The AOA strain *N. gargensis* exhibited about 3–5 times higher RAN biotransformation rates and slightly higher MIA biotransformation rates than those of the two AOBs when grown with the same ammonium concentration at their optimal growth temperatures (Table 1). This could be due to the higher substrate affinities of the responsible enzyme(s). It is known that the ammonia affinity of archaeal AMO is substantially higher than that of the bacterial counterpart.[35,36] Nevertheless, we are aware that the faster biotransformation rates observed in the *N. gargensis* culture could also be partly or even mainly caused by the higher growth temperature for *N. gargensis*. For a more environmentally relevant comparison, the rates should be corrected using the temperature correction factor (Q_{10}, for a

DOI: 10.1021/acs.est.5b06016
Environ. Sci. Technol. 2016, 50, 4682–4692

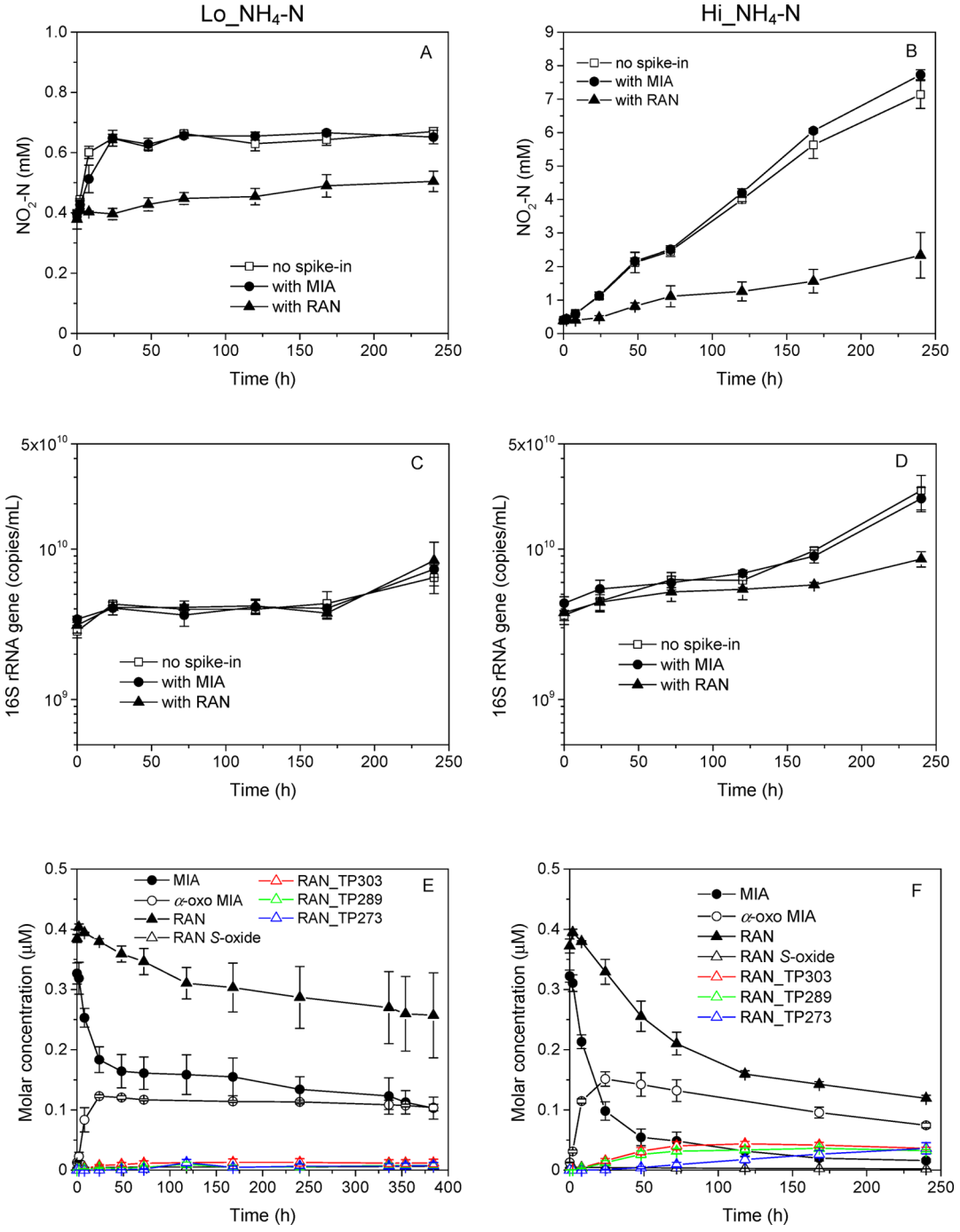

Figure 3. Comparison of MIA and RAN biotransformation by *N. gargensis* between Lo_NH_4-N and Hi_NH_4-N (A, B: nitrite production. Note: different *y* scales are used. C, D: cell growth of *N. gargensis* as measured by qPCR. E, F: biotransformation and TP formation of MIA and RAN, respectively. Note: concentrations of α-oxo MIA, RAN_TP303, TP289, and TP273 were estimated using peak areas and the calibration curve of the corresponding parent compound assuming that TPs have the same ionization efficiency as their parent compounds).

10° temperature difference), which are reaction- and culture/enzyme-specific. Horak et al. found no temperature effect on ammonia oxidation by an AOA-dominated natural marine community within a temperature range of 8−20 °C (Q_{10} = 1.0), whereas higher Q_{10} values for some AOB cultures in soil communities were determined (2.5−17.6, temperature range 5−20 °C).[37] A Q_{10} value of 2.2 was set by default for general evaluation of pesticide degradation in soil.[38] However, Q_{10} values between 28 and 46 °C for MIA and RAN biotransformation by *N. gargensis* are not available. Thus, the extent to which the difference in growth temperatures contributes to the faster biotransformation rates for the AOA strain is uncertain.

Transformation Product Identification. By suspect screening, we found one major MIA TP candidate during MIA biotransformation by both AOA and AOB, with an exact mass of [M + H] at 279.1492 (designated "TP279") and a formula of $C_{18}H_{18}N_2O$ (−2H+O from MIA). Among all possible structures (Figure S9A), we identified TP279 as oxo MIA according to the MS^2 (Figure S10) and MS^3 (Table S4)

DOI: 10.1021/acs.est.5b06016
Environ. Sci. Technol. 2016, 50, 4682−4692

spectra. The likelihood of the three possible oxo MIA structures was 1-oxo > 4-oxo > 3-oxo MIA. Because all of the three positions are at the α-C adjacent to the N of a tertiary amine group, we designate TP279 as α-oxo MIA (Figure 1) (detailed structure analysis is reported in SI section S6). Regarding other known MIA TPs, MIA *N*-oxide was only detected at levels of less than 10% of added MIA, and desmethylmianserin was not detected. MPs may also undergo abiotic nitration mediated by the biogenic nitrite from ammonia oxidation.[39] However, the abiotic nitration of MIA and RAN was not occurring, as neither nitrated MIA nor nitrated RAN was detected. According to estimated α-oxo MIA concentrations assuming it had the same ionization efficiency as MIA on LC-MS/MS, α-oxo MIA in both AOA and AOB cultures accounted for the majority (60−80%) of the removed MIA (Figure 1A, Figure 2A,C). Possible reasons for the not fully closed mass balance include (1) the uncertainty of the quantification method for α-oxo MIA; (2) further transformation of α-oxo MIA as observed in *N. gargensis* (Figure 1A); and (3) formation of other TPs.

MIA is biotransformed mainly by aromatic hydroxylation, *N*-demethylation, *N*-oxidation, and *N*-glucuronidation in humans and other mammals.[40,41] Different from all the known MIA TPs, in this study α-oxo MIA was detected, for the first time, as a major TP during MIA oxidation by ammonia oxidizers. We postulate a two-step oxidative reaction from MIA to yield α-oxo MIA: a hydroxylation at the activated C at α position to one of the N atoms in the aliphatic ring to form the unstable α-hydroxylmianserin intermediate, which was then further oxidized to α-oxo MIA (Figure S9B). The first hydroxylation step is typically carried out by monooxygenases, including AMO.[42] The alkyl substituent hydroxylation of alkylbenzenes, a similar oxidative reaction, was carried out by AMO in *Nitrosomonas europaea*, so was the further oxidation of the ethylbenzene hydroxylation product *sec*-phenethyl alcohol to acetophenone.[43] These findings support the speculation that AMO is involved in MIA biotransformation. Nevertheless, different from RAN, which did not exhibit abiotic degradation, α-oxo MIA was also formed in the fresh-medium control abiotically, although at much lower levels than in the biologically active samples. It is thus possible that, under biotic conditions spontaneous oxidation of MIA may have been accelerated by biogenic oxidizing intermediates.

For RAN, by suspect screening, no TP was detected that accounted for more than 10% of RAN removal, including the reported mammalian TPs, RAN *S*-oxide, RAN *N*-oxide, and desmethylranitidine.[44] RAN *S*-oxide was detected, but only at levels less than 1% of the added RAN (Figure 1B, Figure 2B,D). The other two known TPs were not detected at all. Because the low or even nondetectable levels of RAN TPs could be due to their rapid further degradation, the biotransformation of RAN *S*- and *N*-oxide by *N. gargensis* was also examined (SI section S5). Biotransformation rates of the two TPs were similar to that of RAN (Figure S8 and Table S4). If RAN *S*-/*N*-oxides were the major first generation TPs, they would be expected to accumulate during RAN biotransformation. However, no such accumulation was observed, indicating that RAN *S*-oxide was not likely formed in considerable amounts if at all.

By nontarget analysis, we detected three RAN TP candidates (TP273, TP289, and TP303) with exact masses of [M + H] at 273.1263, 289.1212, and 303.1368, respectively (SI section S6). They accounted for 20−30% of total RAN removal based on peak areas (Figures 1B, 2B,D, and 3E,F). This incomplete mass balance could be due to, first, the uncertainty inherent in the semiquantitative approach using peak areas; second, elution of smaller and more polar RAN TPs with the dead volume on the reversed phase HPLC column, which is quite likely given that the retention time of RAN was only 3.5 min on the column used; third, biosorption to active biomass, which cannot be fully excluded, but is less likely as RAN did not adsorb to heat-inactivated biomass. Structure elucidation based on the MS^2 spectra indicated that all three RAN TPs were formed via reactions occurring at the nitroethenamine moiety whereas the rest of the RAN molecule remained untransformed (see details in Figure S11). However, their exact structures could not be further clarified from available MS^2 spectra, resulting in structure elucidation confidence level 3 (insufficient information for one exact structure only) according to Schymanski and co-workers' classification.[45] On the basis of the TP formulas and approximate structures, we hypothesized a RAN biotransformation pathway via a series of redox and hydrolysis reactions, which can occur biologically (Figure S12). The formulas and structures of intermediates in this pathway do not conflict with the fragments detected in the MS^2 spectra.

Cometabolic Biotransformation of MIA and RAN by *N. gargensis*. To determine whether MIA and RAN biotransformation was metabolic or cometabolic, MIA and RAN biotransformation by *N. gargensis* grown on minimal ammonia (Lo_NH_4-N) were compared to that grown on unlimited ammonia (Hi_NH_4-N). In the MIA-added Lo_NH_4-N culture, MIA biotransformation of *N. gargensis* strongly associated with ammonia oxidation activity. The biotransformation occurred during the first 24 h when there was still some ammonia oxidation activity remaining, whereas it became substantially slower and even ceased after ammonia was completely consumed and no more nitrite was formed (Figure 3A,E). In the RAN-added Lo_NH_4-N culture, RAN inhibited ammonia oxidation, resulting in a rather slow and continuous ammonia oxidation instead of rapid depletion after 24 h. We observed that RAN was slowly biotransformed, concomitant with ammonia oxidation activity (Figure 3A,E).

Little cell growth was observed (Figure 3C) in Lo_NH_4-N, and there was no significant difference between the cultures spiked with the chemicals and the no spike-in control. In contrast, in the Hi_NH_4-N controls both MIA and RAN were continuously biotransformed, and cell density increased as sufficient ammonium was supplied (Figure 3B,D,F). These results suggest that MIA and RAN biotransformations were dependent on active ammonia oxidation and both compounds were biotransformed via cometabolism. Consistently, results of previous studies on pure AOB strains, mostly *N. europaea*, have also suggested cometabolic biotransformation of a number of organic pollutants.[9,12,13,46,47] The addition of RAN inhibited ammonia oxidation of *N. gargensis*, but its biotransformation by *N. gargensis* was not very much inhibited (Table 1). It was likely because that RAN competitively inhibited either AMO or other metabolically essential enzymes, and that the affinity of RAN to the inhibited enzyme was higher than that of its primary substrate (e.g., ammonia in the case of AMO).

Proteomic Analysis of *N. gargensis* during MP Biotransformation. We compared the proteomes of *N. gargensis* grown on 2 mM ammonium with the addition of MIA, RAN, venlafaxine (as nonbiotransformed MP control), as well as without any MP addition. We were able to assign an average of 767 distinct proteins with ≥1 peptide from 1887 nonredundant peptides detected in all samples. Protein abundances were calculated according to methods described

DOI: 10.1021/acs.est.5b06016
Environ. Sci. Technol. 2016, 50, 4682−4692

in SI section S7. No statistically significant difference (t test, p = 0.107) was observed between the protein abundances of *N. gargensis* with MIA or RAN addition and those with the addition of nonbiotransformed venlafaxine or with ammonium only. In addition, no individual protein was up- or down-regulated with statistical significance (t test, FDR < 0.05) in the MIA-/RAN-added samples compared to the samples with venlafaxine or with ammonium only. In contrast, in a study on *N. eutrapha* C91, which mixtrophically degraded *p*-cresol using the intermediates as energy source, up-regulation of almost all enzymes in the TCA cycle were observed in the proteome.[14] Therefore, the result that no protein was differentially expressed after addition of MIA or RAN was consistent with a cometabolic biotransformation mechanism of these compounds by *N. gargensis*.

Environmental Relevance. The two compounds biotransformed by *N. gargensis* are both commonly consumed pharmaceuticals. MIA is a second-generation tetracyclic antidepressant that has been widely used in European countries.[48] RAN inhibits stomach acid production and is highly used as gastrointestinal drug worldwide.[49,50] Both compounds have been detected in a variety of aquatic environments at levels of several to hundreds of ng/L.[50,51] Psychiatric drugs like MIA and high-use drugs like RAN can adversely affect aquatic organisms. MIA exhibits some removal by activated sludge via physical (i.e., sorption) and biological processes,[27] and RAN undergoes direct photolysis in surface water.[49] This study provides additional information regarding their potential biological degradation pathways by AOA and thus helps to achieve a better understanding of their environmental fate and potential for transformation product formation.

The *N. gargensis* pure culture tested in this study is a member of the *Thaumarchaeota* soil group I.1b (also referred to as *Nitrososphaera* cluster)[52] and is closely related to many AOA from soils and WWTPs.[18,24,35,36] Because these AOA share many genes with each other and the AMOs of these AOA are also closely related, it seems likely that similar MP biotransformation characteristics as observed for *N. gargensis* will also be found in *Thaumarchaeotes* thriving in soils and WWTPs. More detailed studies using samples from such systems will be necessary to confirm this hypothesis. To complement with the pure culture study, we conducted an inhibition experiment by applying PTIO, a specific AOA inhibitor[53] to a nitrifying activated sludge sampled from a Swiss municipal WWTP (DOM5 as reported elsewhere[15]). The MP biotransformation activities with and without PTIO were compared (SI section S8). Partial inhibition of MIA and RAN biotransformation was observed, together with a concomitant reduced formation of α-oxo MIA (Figure S13). The formation of another MIA TP, MIA *N*-oxide (Figure S13A), as well as the biotransformation of the other eight MPs (data not shown), was not affected. Given the likely presence of a relatively low abundant population of AOA in the investigated sludge community (SI section S8), the slightly inhibited biotransformation of MIA and α-oxo MIA formation by PTIO suggests that AOA might contribute to MIA biotransformation in that WWTP. Interestingly, the three RAN TPs formed by AOAs were not detected, whereas RAN *S*-oxide formation was inhibited by PTIO (Figure S13B). The actual biotransformation reactions by AOAs in the activated sludge community and the inhibition specificity of PTIO need to be examined more thoroughly in future studies.

One should note that the tested AOA and AOB strains only biotransformed two out of the ten MPs, whereas all of the ten MPs underwent biotransformation at various degrees in the tested nitrifying activated sludge (data not shown). In addition, in the nitrifying activated sludge, TPs other than the ones mainly formed by the pure AOA/AOB strains were also detected (i.e., MIA *N*-oxide, RAN *S*-oxide). If we assume that the AOA/AOB in sludge communities may behave similarly as the isolates, it indicates that not all of the MP biotransformation in the sludge can be solely attributed to ammonia oxidizers. This is also supported by a number of inhibition studies on nitrifying activated sludge.[5,9,54]

In summary, this study represents an important step forward to fill the knowledge gap on MP biotransformation by AOA. First, we provide examples (i.e., MIA and RAN) of MP biotransformation by an AOA pure culture, unraveling a new ecosystem service of AOA in natural and engineered environments. Second, we analyzed the TPs, and the MIA TP was formed via oxidative reactions that typically carried out by monooxygenases. Third, we report several observations that point toward cometabolic biotransformation. These findings provide valuable information regarding the biotransformation kinetics, mechanisms, and transformation products by autotrophic ammonia oxidizers, particularly the archaeal group. However, because environmental microbial communities, such as activated sludge in WWTPs consist of different metabolically diverse microorganisms, and ammonia oxidizers are only part of them, it is important and necessary to examine also the roles played by the other microorganisms, such as heterotrophs possessing unspecific monooxygenases, to reach a more comprehensive and curated understanding of MP biotransformation in a complex community.

■ ASSOCIATED CONTENT

Supporting Information

The Supporting Information is available free of charge on the ACS Publications website at DOI: 10.1021/acs.est.5b06016.

Analytical analysis using LC-MS/MS; sorption and abiotic biotransformation experiments; MP biotransformation by *N. gargensis*, *N. nitrosa* Nm90, and *Nitrosomonas* sp. Nm95; estimation of first-order kinetics parameters; biotransformation of RAN *S*-oxide and RAN *N*-oxide by *N. gargensis*; structure elucidation of MIA TP279, RAN_TP273, TP289, and TP303; proteomic analysis of *N. gargensis* during MIA and RAN biotransformation; effects of the inhibitor PTIO on MIA and RAN biotransformation by nitrifying activated sludge from a Swiss municipal WWTP (PDF).

■ AUTHOR INFORMATION

Corresponding Author

*Yujie Men. Address: 3209 Newmark Civil Engineering Laboratory, MC-250 205 North Mathews Ave., Urbana, IL 61801-2352, USA. Email: ymen2@illinois.edu. Phone: (217) 244-8259.

Notes

The authors declare no competing financial interest.

■ ACKNOWLEDGMENTS

Y.M., D.E.H., D.R.J., and K.F. were supported by Swiss National Science Foundation via the SNF project (CR23I2_140698). P.H. and M.W. were supported by the

DOI: 10.1021/acs.est.5b06016
Environ. Sci. Technol. 2016, 50, 4682−4692

European Research Council via the Advanced Grant project (NITRICARE 294343). We acknowledge Heinz Singer and Dr. Emma Schymanski from the Department of Environmental Chemistry, Eawag, for the LC-MS/MS analysis, Dr. Samuel Derrer from Eawag for the TP synthesis, Dr. Martin von Bergen and Dr. Hans Richnow from the Department of Proteomics and the Department of Isotope Biogeochemistry, Helmholtz-Center for Environment Research Center, UFZ Leipzig, for proteomic LC-MS/MS measurement. Special thanks to Rani Bakkour for his kind help on the abstract art.

REFERENCES

(1) Fenner, K.; Canonica, S.; Wackett, L. P.; Elsner, M. Evaluating pesticide degradation in the environment: blind spots and emerging opportunities. *Science* **2013**, *341*, 752−758.
(2) Luo, Y.; Guo, W.; Ngo, H. H.; Nghiem, L. D.; Hai, F. I.; Zhang, J.; Liang, S.; Wang, X. C. A review on the occurrence of micropollutants in the aquatic environment and their fate and removal during wastewater treatment. *Sci. Total Environ.* **2014**, *473*−*474*, 619−641.
(3) Estevez, E.; Cabrera, M. D.; Molina-Diaz, A.; Robles-Molina, J.; Palacios-Diaz, M. D. Screening of emerging contaminants and priority substances (2008/105/EC) in reclaimed water for irrigation and groundwater in a volcanic aquifer (Gran Canaria, Canary Islands, Spain). *Sci. Total Environ.* **2012**, *433*, 538−546.
(4) Fernandez-Fontaina, E.; Omil, F.; Lema, J. M.; Carballa, M. Influence of nitrifying conditions on the biodegradation and sorption of emerging micropollutants. *Water Res.* **2012**, *46*, 5434−5444.
(5) Tran, N. H.; Urase, T.; Kusakabe, O. The characteristics of enriched nitrifier culture in the degradation of selected pharmaceutically active compounds. *J. Hazard. Mater.* **2009**, *171*, 1051−1057.
(6) Batt, A. L.; Kim, S.; Aga, D. S. Enhanced biodegradation of iopromide and trimethoprim in nitrifying activated sludge. *Environ. Sci. Technol.* **2006**, *40*, 7367−7373.
(7) Rattier, M.; Reungoat, J.; Keller, J.; Gernjak, W. Removal of micropollutants during tertiary wastewater treatment by biofiltration: Role of nitrifiers and removal mechanisms. *Water Res.* **2014**, *54*, 89−99.
(8) Li, F.; Jiang, B.; Nastold, P.; Kolvenbach, B. A.; Chen, J.; Wang, L.; Guo, H.; Corvini, P. F.; Ji, R. Enhanced transformation of tetrabromobisphenol a by nitrifiers in nitrifying activated sludge. *Environ. Sci. Technol.* **2015**, *49*, 4283−4292.
(9) Khunjar, W. O.; Mackintosh, S. A.; Skotnicka-Pitak, J.; Baik, S.; Aga, D. S.; Love, N. G. Elucidating the relative roles of ammonia oxidizing and heterotrophic bacteria during the biotransformation of 17α-Ethinylestradiol and Trimethoprim. *Environ. Sci. Technol.* **2011**, *45*, 3605−3612.
(10) Roh, H.; Subramanya, N.; Zhao, F.; Yu, C. P.; Sandt, J.; Chu, K. H. Biodegradation potential of wastewater micropollutants by ammonia-oxidizing bacteria. *Chemosphere* **2009**, *77*, 1084−1089.
(11) Shi, J.; Fujisawa, S.; Nakai, S.; Hosomi, M. Biodegradation of natural and synthetic estrogens by nitrifying activated sludge and ammonia-oxidizing bacterium *Nitrosomonas europaea*. *Water Res.* **2004**, *38*, 2323−2330.
(12) Chang, S. W.; Hyman, M. R.; Williamson, K. J. Cooxidation of naphthalene and other polycyclic aromatic hydrocarbons by the nitrifying bacterium, *Nitrosomonas europaea*. *Biodegradation* **2002**, *13*, 373−381.
(13) Tran, N. H.; Urase, T.; Ngo, H. H.; Hu, J.; Ong, S. L. Insight into metabolic and cometabolic activities of autotrophic and heterotrophic microorganisms in the biodegradation of emerging trace organic contaminants. *Bioresour. Technol.* **2013**, *146*, 721−731.
(14) Kjeldal, H.; Pell, L.; Pommerening-Roser, A.; Nielsen, J. L. Influence of *p*-cresol on the proteome of the autotrophic nitrifying bacterium *Nitrosomonas eutropha* C91. *Arch. Microbiol.* **2014**, *196*, 497−511.
(15) Helbling, D. E.; Johnson, D. R.; Honti, M.; Fenner, K. Micropollutant biotransformation kinetics associate with WWTP process parameters and microbial community characteristics. *Environ. Sci. Technol.* **2012**, *46*, 10579−10588.
(16) Wells, G. F.; Park, H. D.; Yeung, C. H.; Eggleston, B.; Francis, C. A.; Criddle, C. S. Ammonia-oxidizing communities in a highly aerated full-scale activated sludge bioreactor: betaproteobacterial dynamics and low relative abundance of Crenarchaea. *Environ. Microbiol.* **2009**, *11*, 2310−2328.
(17) Gao, J. F.; Luo, X.; Wu, G. X.; Li, T.; Peng, Y. Z. Quantitative analyses of the composition and abundance of ammonia-oxidizing archaea and ammonia-oxidizing bacteria in eight full-scale biological wastewater treatment plants. *Bioresour. Technol.* **2013**, *138*, 285−296.
(18) Limpiyakorn, T.; Furhacker, M.; Haberl, R.; Chodanon, T.; Srithep, P.; Sonthiphand, P. *amoA*-encoding archaea in wastewater treatment plants: a review. *Appl. Microbiol. Biotechnol.* **2013**, *97*, 1425−1439.
(19) Sauder, L. A.; Peterse, F.; Schouten, S.; Neufeld, J. D. Low-ammonia niche of ammonia-oxidizing archaea in rotating biological contactors of a municipal wastewater treatment plant. *Environ. Microbiol.* **2012**, *14*, 2589−2600.
(20) Sayavedra-Soto, L. A.; Hamamura, N.; Liu, C. W.; Kimbrel, J. A.; Chang, J. H.; Arp, D. J. The membrane-associated monooxygenase in the butane-oxidizing Gram-positive bacterium *Nocardioides* sp. strain CF8 is a novel member of the AMO/PMO family. *Environ. Microbiol. Rep.* **2011**, *3*, 390−396.
(21) Martens-Habbena, W.; Berube, P. M.; Urakawa, H.; de la Torre, J. R.; Stahl, D. A. Ammonia oxidation kinetics determine niche separation of nitrifying Archaea and Bacteria. *Nature* **2009**, *461*, 976−979.
(22) Hatzenpichler, R.; Lebedeva, E. V.; Spieck, E.; Stoecker, K.; Richter, A.; Daims, H.; Wagner, M. A moderately thermophilic ammonia-oxidizing crenarchaeote from a hot spring. *Proc. Natl. Acad. Sci. U. S. A.* **2008**, *105*, 2134−2139.
(23) Palatinszky, M.; Herbold, C.; Jehmlich, N.; Pogoda, M.; Han, P.; von Bergen, M.; Lagkouvardos, I.; Karst, S. M.; Galushko, A.; Koch, H.; Berry, D.; Daims, H.; Wagner, M. Cyanate as an energy source for nitrifiers. *Nature* **2015**, *524*, 105−108.
(24) Mussmann, M.; Brito, I.; Pitcher, A.; Sinninghe Damste, J. S.; Hatzenpichler, R.; Richter, A.; Nielsen, J. L.; Nielsen, P. H.; Muller, A.; Daims, H.; Wagner, M.; Head, I. M. Thaumarchaeotes abundant in refinery nitrifying sludges express *amoA* but are not obligate autotrophic ammonia oxidizers. *Proc. Natl. Acad. Sci. U. S. A.* **2011**, *108*, 16771−16776.
(25) Koops, H. P.; Bottcher, B.; Möller, U. C.; Pommereningroser, A.; Stehr, G. Classification of 8 new species of ammonia-oxidizing bacteria: *Nitrosomonas communis* sp. nov., *Nitrosomonas* ureae sp. nov., *Nitrosomonas* aestuarii sp. nov., *Nitrosomonas* marina sp. nov., *Nitrosomonas nitrosa* sp. nov., *Nitrosomonas eutropha* sp. nov., *Nitrosomonas oligotropha* sp. nov. and *Nitrosomonas halophila* sp. nov. *J. Gen. Microbiol.* **1991**, *137*, 1689−1699.
(26) Wahman, D. G.; Katz, L. E.; Speitel, G. E., Jr. Cometabolism of trihalomethanes by *Nitrosomonas europaea*. *Appl. Environ. Microbiol.* **2005**, *71*, 7980−7986.
(27) Gulde, R.; Helbling, D. E.; Scheidegger, A.; Fenner, K. pH-dependent biotransformation of ionizable organic micropollutants in activated sludge. *Environ. Sci. Technol.* **2014**, *48*, 13760−13768.
(28) Helbling, D. E.; Hollender, J.; Kohler, H. P.; Fenner, K. Structure-based interpretation of biotransformation pathways of amide-containing compounds in sludge-seeded bioreactors. *Environ. Sci. Technol.* **2010**, *44*, 6628−6635.
(29) Stoob, K.; Singer, H. P.; Goetz, C. W.; Ruff, M.; Mueller, S. R. Fully automated online solid phase extraction coupled directly to liquid chromatography-tandem mass spectrometry quantification of sulfonamide antibiotics, neutral and acidic pesticides at low concentrations in surface waters. *J. Chromatogr. A* **2005**, *1097*, 138−147.
(30) Huntscha, S.; Singer, H. P.; McArdell, C. S.; Frank, C. E.; Hollender, J. Multiresidue analysis of 88 polar organic micropollutants in ground, surface and wastewater using online mixed-bed multilayer solid-phase extraction coupled to high performance liquid chromatog-

DOI: 10.1021/acs.est.5b06016
Environ. Sci. Technol. 2016, 50, 4682−4692

raphy-tandem mass spectrometry. *J. Chromatogr. A* **2012**, *1268*, 74−83.
(31) Krauss, M.; Singer, H.; Hollender, J. LC-high resolution MS in environmental analysis: from target screening to the identification of unknowns. *Anal. Bioanal. Chem.* **2010**, *397*, 943−951.
(32) Gulde, R.; Meier, U.; Schymanski, E. L.; Kohler, H. E.; Helbling, D. E.; Derrer, S.; Rentsch, D.; Fenner, K. Systematic Exploration of Biotransformation Reactions of Amine-Containing Micropollutants in Activated Sludge. *Environ. Sci. Technol.* **2016**, *50*, 2908−2920.
(33) Strickland, J. D. H.; Parsons, T. R. *A Practical Handbook of Seawater Analysis*; Bulletin 167; Fisheries Research Board of Canada: Ottawa, 1972.
(34) Kandeler, E.; Gerber, H. Short-term assay of soil urease activity using colorimetric determination of ammonium. *Biol. Fertil. Soils* **1988**, *6*, 68−72.
(35) Stahl, D. A.; de la Torre, J. R. Physiology and diversity of ammonia-oxidizing archaea. *Annu. Rev. Microbiol.* **2012**, *66*, 83−101.
(36) Pester, M.; Schleper, C.; Wagner, M. The Thaumarchaeota: an emerging view of their phylogeny and ecophysiology. *Curr. Opin. Microbiol.* **2011**, *14*, 300−306.
(37) Horak, R. E.; Qin, W.; Schauer, A. J.; Armbrust, E. V.; Ingalls, A. E.; Moffett, J. W.; Stahl, D. A.; Devol, A. H. Ammonia oxidation kinetics and temperature sensitivity of a natural marine community dominated by Archaea. *ISME J.* **2013**, *7*, 2023−2033.
(38) EFSA PPR Panel (EFSA Panel on Plant Protection Products and their Residues) Opinion of the Scientific Panel on Plant protection products and their residues (PPR) related to the default Q_{10} value used to describe the temperature effect on transformation rates of pesticides in soil. *EFSA J.* **2006**, *322*, DOI:10.2903/j.efsa.
(39) Sun, Q.; Li, Y.; Chou, P. H.; Peng, P. Y.; Yu, C. P. Transformation of bisphenol A and alkylphenols by ammonia-oxidizing bacteria through nitration. *Environ. Sci. Technol.* **2012**, *46*, 4442−4448.
(40) de Jongh, G. D.; van den Wildenberg, H. M.; Nieuwenhuyse, H.; van der Veen, F. The metabolism of mianserin in women, rabbits, and rats: identification of the major urinary metabolites. *Drug Metab. Dispos.* **1981**, *9*, 48−53.
(41) Roberts, P.; Kitteringham, N. R.; Park, B. K. Species differences in the activation of mianserin to a cytotoxic metabolite. *Drug Metab. Dispos.* **1991**, *19*, 841−843.
(42) Silverman, R. B. *The organic chemistry of enzyme-catalyzed reactions*. Rev. ed.; Academic Press: San Diego, U.S.A., 2002.
(43) Keener, W. K.; Arp, D. J. Transformations of aromatic compounds by *Nitrosomonas europaea*. *Appl. Environ. Microbiol.* **1994**, *60*, 1914−1920.
(44) Cross, D. M.; Bell, J. A.; Wilson, K. Kinetics of ranitidine metabolism in dog and rat isolated hepatocytes. *Xenobiotica* **1995**, *25*, 367−375.
(45) Schymanski, E. L.; Jeon, J.; Gulde, R.; Fenner, K.; Ruff, M.; Singer, H. P.; Hollender, J. Identifying small molecules via high resolution mass spectrometry: communicating confidence. *Environ. Sci. Technol.* **2014**, *48*, 2097−2098.
(46) Ely, R. L.; Williamson, K. J.; Hyman, M. R.; Arp, D. J. Cometabolism of chlorinated solvents by nitrifying bacteria: kinetics, substrate interactions, toxicity effects, and bacterial response. *Biotechnol. Bioeng.* **1997**, *54*, 520−534.
(47) Maestre, J. P.; Wahman, D. G.; Speitel, G. E., Jr. Monochloramine cometabolism by *Nitrosomonas europaea* under drinking water conditions. *Water Res.* **2013**, *47*, 4701−4709.
(48) van der Ven, K.; Keil, D.; Moens, L. N.; Van Leemput, K.; van Remortel, P.; De Coen, W. M. Neuropharmaceuticals in the environment: mianserin-induced neuroendocrine disruption in zebrafish (Danio rerio) using cDNA microarrays. *Environ. Toxicol. Chem.* **2006**, *25*, 2645−2652.
(49) Latch, D. E.; Stender, B. L.; Packer, J. L.; Arnold, W. A.; McNeill, K. Photochemical fate of pharmaceuticals in the environment: cimetidine and ranitidine. *Environ. Sci. Technol.* **2003**, *37*, 3342−3350.
(50) Isidori, M.; Parrella, A.; Pistillo, P.; Temussi, F. Effects of ranitidine and its photoderivatives in the aquatic environment. *Environ. Int.* **2009**, *35*, 821−825.
(51) Giebultowicz, J.; Nalecz-Jawecki, G. Occurrence of antidepressant residues in the sewage-impacted Vistula and Utrata rivers and in tap water in Warsaw (Poland). *Ecotoxicol. Environ. Saf.* **2014**, *104*, 103−109.
(52) Pester, M.; Rattei, T.; Flechl, S.; Grongroft, A.; Richter, A.; Overmann, J.; Reinhold-Hurek, B.; Loy, A.; Wagner, M. *amoA*-based consensus phylogeny of ammonia-oxidizing archaea and deep sequencing of *amoA* genes from soils of four different geographic regions. *Environ. Microbiol.* **2012**, *14*, 525−539.
(53) Martens-Habbena, W.; Qin, W.; Horak, R. E.; Urakawa, H.; Schauer, A. J.; Moffett, J. W.; Armbrust, E. V.; Ingalls, A. E.; Devol, A. H.; Stahl, D. A. The production of nitric oxide by marine ammonia-oxidizing archaea and inhibition of archaeal ammonia oxidation by a nitric oxide scavenger. *Environ. Microbiol.* **2015**, *17*, 2261−2274.
(54) Yu, C. P.; Roh, H.; Chu, K. H. 17β-estradiol-degrading bacteria isolated from activated sludge. *Environ. Sci. Technol.* **2007**, *41*, 486−492.

DOI: 10.1021/acs.est.5b06016
Environ. Sci. Technol. 2016, 50, 4682−4692